FULL TITLE

Sexually dimorphic changes in the endocrine pancreas and skeletal muscle in young adulthood following intra-amniotic IGF-I treatment of growth-restricted fetal sheep

Authors list

Emma J. Buckels,[1] Frank H. Bloomfield,[1] Mark H. Oliver,[1] Ana-Mishel Spiroski,[1] Jane E. Harding,[1] and Anne L. Jaquiery[1]

Brief itemized list of how each author contributed to the study

Study conception and design: EJB, FHB, MHO, AMS, JEH, ALJ

Acquisition of data: EJB, AMS

Analysis and interpretation of data: EJB, ALJ

Drafting of manuscript: EJB, ALJ

Critical revision: EJB, FHB, MHO, AMS, JEH, ALJ

Affiliations (all departments/institutions where the work was done), with city and country

[1]The Liggins Institute, University of Auckland, Auckland, New Zealand

Running head

Pancreas and muscle following IGF-I treatment of FGR lambs

Address for correspondence

Corresponding author: Anne L. Jaquiery: Liggins Institute, University of Auckland, Private Bag 92019, Auckland, New Zealand. Email: a.jaquiery@auckland.ac.nz

Supplemental Material available at:

URL: https://figshare.com/s/2d6be3e98052adba7f00

DOI: https://doi.org/10.17608/k6.auckland.14337299

ABSTRACT (250 WORDS)

Fetal growth restriction (FGR) is associated with decreased insulin secretory capacity and decreased insulin sensitivity in muscle in adulthood. We investigated whether intra-amniotic IGF-I treatment in late gestation mitigated the adverse effects of FGR on the endocrine pancreas and skeletal muscle at 18-months of age. Singleton-bearing ewes underwent uterine artery embolization between 103-107 days' gestational age, followed by five once-weekly intra-amniotic injections of 360 μg IGF-I (FGRI) or saline (FGRS), and were compared to an un-manipulated control group (CON). We measured offspring pancreatic endocrine cell mass and pancreatic and skeletal muscle mRNA expression at 18-months of age (n=7-9/sex/group). Total α-cell mass was increased ~225% in FGRI males vs. CON and FGRS males, while β-cell mass was not different between groups of either sex. Pancreatic mitochondria-related mRNA expression was increased in FGRS females vs. CON (NRF1, MTATP6, UCP2), and FGRS males vs. CON (TFAM, NRF1, UCP2), but was largely unchanged in FGRI males vs. CON. In skeletal muscle, mitochondria-related mRNA expression was decreased in FGRS females vs. CON (PPARGC1A, TFAM, NRF1, UCP2, MTATP6), FGRS males vs. CON (NRF1 and UCP2), and FGRI females vs. CON (TFAM and UCP2), with only MTATP6 expression decreased in FGRI males vs. CON. Although the window during which IGF-I treatment was delivered was limited to the final five weeks of gestation, IGF-I therapy of FGR altered the endocrine pancreas and skeletal muscle in a sex-specific manner in young adulthood.

Keywords (Three to five keywords)

Fetal therapy

Intrauterine intervention

Developmental origins of health and disease

Glucose-stimulated insulin secretion

Insulin signaling

NEW AND NOTEWORTHY

Fetal growth restriction (FGR) is associated with compromised metabolic function throughout adulthood. Here, we explored the long-term effects of fetal IGF-I therapy on the adult pancreas and skeletal muscle. This is the first study demonstrating that IGF-I therapy of FGR has sex-specific long-term effects at both the tissue and molecular level on metabolically active tissues in adult sheep.

INTRODUCTION

Fetal growth restriction (FGR), the failure of a fetus to reach its intrauterine growth potential, is estimated to affect 5-10% of all pregnancies (1). FGR is associated with perinatal morbidity, stillbirth, and perinatal death (2-5). Placental insufficiency, a common cause of FGR (1), compromises placental transfer of nutrients from the maternal circulation into the fetal circulation, resulting in a hypoglycemic and hypoxic intrauterine environment (6). Despite an urgent need, there are currently no clinically proven treatments to increase fetal growth or improve perinatal outcomes in pregnancies diagnosed with FGR (7).

Beyond the perinatal period, FGR is associated with an increased risk of developing metabolic disease in adulthood, including obesity and type 2 diabetes mellitus (T2DM) (8, 9). T2DM develops when insulin secretion is insufficient to overcome insulin resistance in target organs, such as skeletal muscle, the liver, and adipose tissue, resulting in chronically elevated circulating glucose concentrations. Nutritional insults experienced by the growth-restricted fetus can permanently alter the structure and function of critical metabolically-active organs, such as the endocrine pancreas and skeletal muscle (10). Studies in FGR sheep demonstrate decreased β-cell mass at birth (11). Given the limited ability of β-cell mass to expand in response to increased metabolic demand later in life, this may have implications for metabolic health in adulthood (12). Decreased β-cell mass is commonly associated with impaired insulin secretion and T2DM (13), presumed to be due to a smaller population of β-cells available to secrete insulin. In addition to its effects on endocrine cell populations, FGR decreases the expression of components of the glucose-stimulated insulin secretion (GSIS) pathway and mitochondria number and function (figure 1A), affecting the ability of the β-cell to mount a sufficient insulin response following nutritional stimulation (11, 14, 15). Low lean mass at birth following FGR establishes a life-long deficit of lean mass (16, 17, 18), which is associated with decreased expression in skeletal muscle of mRNA and proteins involved with insulin signaling and mitochondria number and function (figure 1B) (19-23). These changes are associated with decreased insulin sensitivity (24) and, therefore, potentially the risk of developing T2DM.

Sex-specific responses to an early-life nutritional insult have been shown in various animal experimental studies and human observational cohorts in which fetuses were exposed to nutritional insults or toxins (25). These studies demonstrate that males typically have poorer outcomes than females when exposed to an adverse intrauterine environment, but the mechanism by which sex influences these outcomes remains unclear (25, 26).

Insulin-like growth factor (IGF)-I administered into the amniotic fluid has been shown to increase growth in FGR sheep fetuses with placental insufficiency in a sex-specific manner, without affecting perinatal mortality in either sex (27-33). Intra-amniotic IGF-I treatment does not increase placental size (27, 28) but increases fetal growth and placental expression of amino acid transporters (27). The growth-promoting effect of IGF-I treatment is greater in female fetuses, and appears to have a minimal effect on birthweight in males (29). Patterns of postnatal growth also differ between sexes, with IGF-I-treated adult females, but not males, being leaner than controls (29). In early adulthood (18-months of age), the insulin response throughout an intravenous glucose tolerance test (ivGTT) was decreased in growth-restricted females independent of IGF-I treatment, despite having a glucose response similar to normally grown controls (33). Glucose disposition index (DI), calculated by multiplying insulin sensitivity during an hyperglycemic clamp (HGC) with first-phase insulin secretion from an ivGTT, was decreased by 50% in growth-restricted females compared to controls, but this reduction was not seen in IGF-I-treated females. Conversely, growth-restricted males had increased glucose response and decreased insulin secretion relative to glucose response throughout an ivGTT compared to controls; this effect was absent in males treated with IGF-I. Insulin sensitivity was similar between groups in both sexes at this age (33). Therefore, both females and males exposed to FGR had decreased insulin secretion following a glucose challenge and, in males only, insulin secretion was similar to normally-grown males following treatment with IGF-I.

We hypothesized that, at 18-months of age, sheep that experienced FGR would have sex-specific alterations in endocrine islet cell composition, specifically decreased β-cell mass, decreased expression of mRNA transcripts associated with glucose-stimulated insulin secretion (GSIS) in the pancreas and with insulin signaling in skeletal muscle; that these effects would be sex-specific; and that intra-amniotic IGF-I treatment would ameliorate any changes observed, also in a sex-specific manner.

METHODS

Ethics statement.

Animal experiments were approved by the University of Auckland Animal Ethics Committee (approval numbers R628 and R874), and all experiments were conducted following the National Animal Ethics Advisory Committee guidelines and institutional standard operating procedures. Animal studies are reported in compliance with the ARRIVE guidelines (34).

Experimental animals.

Experimental animals were generated as previously described (29). Briefly, singleton-bearing ewes were randomized to a control (CON) or FGR group. FGR ewes underwent surgery between 97-100 days gestational age (dGA) to insert chronic indwelling polyvinyl chloride catheters into fetal and maternal arteries and the amniotic cavity. FGR was induced by bilateral maternal uterine artery embolization using Superose 12 microspheres (GE Healthcare, Little Chalfont, United Kingdom). Embolization was performed twice daily between 103-107 dGA, titrated against fetal blood gases. Fetuses were then randomized to receive either 360 μg human recombinant IGF-I (FGRI; Genentech, San Francisco, California, USA), or an equivolume dose of 3.6 mL sterile saline (FGRS), via weekly intra-amniotic injection between 107-135 dGA. CON ewes did not undergo surgery, embolization, or treatment, but were maintained alongside experimental ewes throughout the study.

Lambs were born vaginally and individually housed with their ewe. At two-weeks of age, ewe-lamb pairs were transitioned to a group pen, and at three weeks of age, lambs were transitioned onto pasture. At three months of age, lambs were weaned and maintained in a same-sex herd. Males were not castrated. The offspring were maintained according to standard farm protocols until 18-months of age. We have previously reported experimental animal use, fetal and perinatal losses (29), and sheep losses to 18-months of age (33).

Physiological testing.

At 18-months of age, a random number generator was used to select a subset of adult sheep to undergo physiological testing. These tests included an intravenous glucose tolerance test (ivGTT), an HGC, and an epinephrine stimulation test, which have been described previously (33). A controlled internal drug release device (CIDR) containing 3 mg progesterone (Pfizer,

Auckland, New Zealand) was inserted intravaginally into ewes three days before the start of physiological testing to synchronize estrus. Testing was conducted with the CIDR *in situ*.

Tissue collection.

Five to six days after completing physiological testing, sheep were fasted overnight and then euthanized with an intravenous bolus of sodium pentobarbitone (100-120 $mg.kg^{-1}$; Provet, Auckland, New Zealand). Pancreata were harvested and weighed. Two 1 cm medial strips of pancreata were bisected. Each strip contained head, body, and tail regions of the pancreas. One strip was snap-frozen in liquid nitrogen, and the other was preserved in 4% paraformaldehyde. A 1 cm^3 section of the *vastus lateralis* muscle was snap-frozen in liquid nitrogen, and frozen samples were stored at -80ºC until analysis. The vastus lateralis was chosen for our study as it is of mixed fiber type; it is the largest muscle in the quadriceps and, therefore, effects of perturbations in this muscle will be proportionally greater. Subsequent molecular analyses were performed on tissues from experimental animals that had undergone the full complement of physiological testing at 18-months of age (female: CON, n=8; FGRS, n=9; FGRI, n=8; male: CON, n=8; FGRS, n=7; FGRI, n=8).

Immunohistochemistry.

For each pancreas, serial 5 μm tissue sections were cut from paraffin-embedded fixed tissue. Five sections, 100 μm apart, were selected for immunostaining. Immunofluorescent staining was performed with antibodies against insulin, glucagon, and somatostatin, to determine β-cell, α-cell, and δ-cell area, as previously described (35-37). Mature endocrine hormones were labeled with guinea pig anti-porcine insulin (1:500; Dako, Carpinteria, California), mouse anti-porcine glucagon (1:500; Sigma Aldrich, St Louis, Missouri), and rabbit anti-human somatostatin (1:500; Dako). Primary antibodies were detected with anti-guinea pig IgG Alexa Fluor 647, anti-mouse IgG Alexa Fluor 488, and anti-rabbit IgG Alexa Fluor 594 secondary antibodies (all at 1:400, all raised in goat; Invitrogen, Carlsbad, California, USA). Cell nuclei were stained with 0.5 μg/mL 6-diamidino-2-phenylindole (DAPI; Sigma Aldrich, St Louis, Missouri, USA). Sections were mounted with ProLong Gold Antifade Reagent (Life Technologies, California, USA).

Sections were visualized at 200× magnification using an AxioImager Z2 microscope (Carl Zeiss Microscopy, Jena, Germany), connected to a Metafer4 Slide Scanning Platform (MetaSystems, Altlussheim, Germany) to generate whole-slide images. Images were analyzed using an automated workflow in Fiji (38) on each field of view image. Individual fields of view were

manually checked for staining artifacts and excluded if detected. Areas that were positive for insulin, glucagon, and somatostatin were used to calculate β-cell, α-cell, and δ-cell mass, respectively, by multiplying the area positive for each cell type (μm^2), by the pancreas weight (mg), normalized to the total amount of tissue scanned on each slide (μm^2) (35). Total islet cell area was calculated by adding cell mass calculated for each islet cell type, and relative islet cell mass was calculated as the mass of each islet cell type divided by total islet cell mass (35). We did not measure pancreatic-peptide (PP), a marker for PP-cells, as this cell type represents approximately 1-2% of islet cell mass in the sheep (35), and less than 5% in rodent or human islets (39), and therefore has a minimal effect on total islet cell mass.

RNA isolation.

Total RNA was isolated from 25 mg snap-frozen pancreas and 50 mg frozen *vastus lateralis*. Tissues were ground to a fine powder in a liquid nitrogen super-cooled stainless steel mortar and pestle. As the dispersion of endocrine cells throughout the pancreas is unknown, the pancreas was ground in its entirety, and a 25 mg portion was used for RNA isolation. Ground tissue was mixed with 1 mL ice-cold Trizol (Invitrogen, California, USA) in a homogenizer tube. With a T 25 Basic ULTRA-TURRAX power homogenizer (IKA, Staufen, Germany), samples were homogenized for three rounds of 20 seconds at 24,000 rpm, with 20-30 seconds incubation on ice between rounds. An additional round of homogenization was performed if required. The Trizol-tissue solution was transferred into a 2 mL microcentrifuge tube. The remainder of the extraction was performed as per manufacturer's instructions, with the chloroform phase separation step performed twice to avoid phenol contamination. RNA was re-suspended in 50 μL nuclease-free water (Ambion; Life Technologies, California, USA). Samples were stored at -80°C until RNA quality control was performed.

RNA quality control.

RNA samples were thawed on ice, and all quality control processes were performed within the same freeze-thaw cycle. Isolated RNA was quantified with a Qubit RNA HS Assay Kit (Life Technologies, California, USA). A 1 μL sample was diluted 1:20 with nuclease-free water (Ambion; Life Technologies, California, USA), and 1 μL of this dilution was mixed with 199 μL Qubit working solution. The assay was performed as per the manufacturer's instructions. All samples had RNA concentrations above 0.200 μg/μL. RNA purity assessed with a NanoDrop 1000 Spectrophotometer (Thermo Scientific, Massachusetts, USA). All samples had a 260/280 absorbance ratio between 1.8 and 2.2. RNA integrity was measured with RNA 6000 Nano Chips

(Agilent Technologies, California, USA). Each assay was performed according to the manufacturer's instructions, using the total eukaryotic RNA program. RNA derived from skeletal muscle samples had RIN values between 7 and 9. RNA derived from whole pancreas demonstrated a similar level of degradation (RIN values between 2 and 5), not uncommon in pancreata due to high ribonuclease concentration in the exocrine pancreas and the challenges of achieving rapid preservation during tissue collection. However, RT-qPCR is more tolerant of RNA degradation than other methods of measuring mRNA expression, such as next-generation RNA sequencing, and we normalized mRNA expression to a panel of three reference genes, which has been shown to minimize the impact of mRNA degradation (40). Additionally, all target amplicons were shorter than 105 base pairs in length; amplicons less than 250 base pairs are independent of RNA quality (41).

Generation of cDNA and RT-qPCR.

For each sample, 2.5 μg of total RNA underwent DNase I treatment (Invitrogen, California, USA), according to the manufacturer's instructions. Subsequently, cDNA was synthesized with a SuperScript VILO cDNA Synthesis Kit (Invitrogen, California, USA).

Real-time quantitative reverse transcription PCR (RT-qPCR) was performed using an ABI 7900HT Fast Real-Time PCR System (Applied Biosystems, California, USA) for samples derived from pancreata, and with a QuantStudio 6 Flex Real-Time PCR System (Applied Biosystems) for samples derived from skeletal muscle. Two systems were used as the 7900HT system was upgraded between studies. Standard cycling parameters were used (50°C for two minutes, 95°C for 10 minutes, followed by 40 cycles of 95°C for 15 seconds followed by 60°C for one minute).

Custom TaqMan Gene Expression Assays were purchased from Applied Biosystems (Life Technologies, California, USA). GenBank (National Center for Biotechnology Information (NCBI)) was searched for the ovine sequences of interest. Alternatively, where no ovine sequence could be found, porcine or bovine sequences that had 100% region homology with the predicted ovine sequences were used. Between 60 and 150 base pairs of the sequence were entered into the Custom TaqMan Assay Design Tool (Life Technologies) for each gene of interest. Due to the limited information available on ovine sequences, no emphasis was placed on designing primers and probes that would span exon-exon borders. Details on where selected genes of interest (listed in supplementary table 1) involved in the GSIS or insulin signaling pathways are depicted in figure 1.

Custom TaqMan Gene Expression Assays were ordered from the recommended primer and probe design outputs (supplementary table 1). All TaqMan probes had FAM fluorescent reporter dyes and were quenched with 5' a molecular-groove binding non-fluorescence quencher (MGBNFQ). To ensure primer specificity, a basic local alignment search tool (BLAST) search was performed for each amplicon (42) to search for homology to alternate sequences. Additionally, a sample of PCR product generated below underwent gel electrophoresis. A 10 μL sample of PCR product was combined with 2 μL bromophenol blue and ran on a 2% agarose gel with 0.01% ethidium bromide in 1xTBE buffer. The appearance of a single band at the expected fragment size for each amplicon was considered acceptable.

mRNA expression was quantified in triplicate singleplex reactions, with each 10 μL reaction volume containing 5 μL TaqMan Gene Expression Master Mix (Applied Biosystems), 900 nmol forward and reverse primer, 200 nmol probe, and 1 μL diluted cDNA. Gene names and primer and probe details can be found in supplementary table 1. A standard curve was performed for each target amplicon. Relative amounts of mRNA expression were quantified using the standard curve method and normalized to the geometric mean of the stable reference mRNA transcripts for each tissue (43). Reference mRNA transcript stability across a random selection of samples was determined by assessing the standard deviation and coefficient of variation across a panel of reference genes. The three most stable reference genes were β-actin, RPL19, and YHWAZ for RNA derived from the pancreas, and β-actin, GAPDH, and PPIA for RNA derived from skeletal muscle.

Statistical analysis.

Pancreatic endocrine cell mass data were analyzed in GraphPad Prism (Version 8.0.2; San Diego, California, USA). Data were checked for normality using the Shapiro-Wilk test and log-transformed when necessary. One-way ANOVA within each sex was used to determine the effects of FGR and intra-amniotic treatment of FGR with IGF-I, and Tukey *post hoc* testing was applied where appropriate.

Regression analyses were used to assess the relationship between continuous variables. A probability of $p<0.05$ was considered statistically significant. These data are presented as mean and SEM.

For mRNA expression data, relative expression was calculated with the real-time PCR efficiency of each primer-probe set and normalized to the geometric mean of three stable reference genes (43). Data were analyzed as fold change in mRNA expression relative to a comparator group. Alpha was set at 0.01, and data are presented as fold change with 99% confidence intervals.

With the exception of the regression analyses, we were interested in the following comparisons for each comparison: (1) CON vs. FGRS, to determine if FGR had any longstanding effects compared to that of control sheep; (2) CON vs. FGRI, to determine whether IGF-I therapy of FGR had potentially returned the phenotype to that of control sheep, and (3) FGRS vs. FGRI, to specifically explore if IGF-I therapy had any effect on the phenotype in FGR sheep.

RESULTS

Birthweight, bodyweight, body composition, and organ weights at 18-months of age.

Perinatal outcomes (29), bodyweight, body composition, and organ weights at 18-months of age (33) have been reported previously. Briefly, FGRS but not FGRI female lambs were lighter at birth than CON female lambs. Conversely, FGRS and FGRI male lambs were smaller than CON male lambs, with no difference between FGRS and FGRI males. Bodyweight and fat mass were similar amongst groups within each sex at 18-months of age. FGRI female sheep had greater lean mass relative to bodyweight compared to CON female sheep, with no difference between FGRS female sheep and FGRI or CON female sheep. There was no difference in lean mass amongst groups for male sheep at 18-months of age. Absolute brain, liver, and pancreas weights were similar between groups within each sex at 18-months of age.

Endocrine cell populations in the pancreas.

In female sheep, FGRS tended to have less total islet cell mass compared to CON ($p=0.099$; table 1 and figure 2), but total β-, and α-cell masses were not different amongst groups. Absolute δ-cell mass was increased in FGRI compared to FGRS females ($p=0.005$). The proportion of β-cell and δ-cell mass relative to total islet cell mass differed amongst groups ($p=0.045$ and $p=0.02$, respectively; table 1 and figure 2) with post-hoc tests demonstrating that female FGRI tended to have an decreased proportion of β-cells compared to CON ($p=0.09$) and FGRS ($p=0.06$), and an increased proportion of δ-cells compared to CON ($p=0.05$) and FGRS ($p=0.03$).

β-cell mass relative to bodyweight was decreased by approximately 30% in FGRS compared to CON females, but this was not statistically significant ($p=0.11$) (table 1). Relative to bodyweight, δ-cell mass was increased in FGRI compared to FGRS ($p=0.003$) and tended to be increased compared to CON ($p=0.06$), while relative α-cell mass was not different amongst groups in females (table 1).

In males, total islet cell mass, β-cell mass, and δ-cell mass were not different amongst groups (table 1). However, in FGRI, total α-cell mass was increased ~225% compared to CON ($p=0.01$) and FGRS ($p=0.01$), and as a proportion of total islet cell mass (vs. CON, $p=0.007$; vs. FGRS, $p=0.07$). Moreover, the ratio of α-cell to β-cell mass was increased in FGRI compared to both CON ($p=0.002$) and FGRS ($p=0.008$). Only α-cell mass relative to bodyweight was increased in FGRI compared to both CON and FGRS male sheep (both $p=0.01$).

340

341 *Correlations between pancreatic endocrine cell mass and physical characteristics.*

342 There were no correlations between birthweight, bodyweight, or lean mass and total islet cell
343 mass, β-cell mass, α-cell mass, or δ-cell mass in any group of either sex except for positive
344 correlations between bodyweight and total islet cell mass in FGRI females (R^2=0.58, p=0.046),
345 bodyweight and β-cell mass in FGRI females (R^2=0.64, p=0.03), and lean mass and δ-cell mass
346 in CON males (R^2=0.68, p=0.02; supplementary figures 1 and 2). Only female FGRI sheep
347 demonstrated a positive correlation between fat mass and total islet cell mass (R^2=0.67, p=0.02)
348 and β-cell mass (R^2=0.76, p=0.01; supplementary figure 1). These correlations were absent in any
349 male group (supplementary figure 2).

350

351 *Correlations between pancreatic endocrine cell mass and responses to ivGTT and HGC.*

352 There were no significant correlations between the glucose or insulin responses throughout an
353 ivGTT and β-cell mass in any group in either female (figure 3A) or male (figure 3B) sheep. Nor
354 were there any correlations between the glucose or insulin response throughout an ivGTT and
355 total islet cell mass, α-cell mass, or δ-cell mass in any group in either sex (data not shown).

356

357 There were no correlations between β-cell mass and the mean steady-state plasma insulin
358 concentration during an HGC, glucose disposition index, or GSIS, in any group in either sex
359 (data not shown).

360

361 *Whole pancreas mRNA expression of genes involved with GSIS and mitochondria number and function.*

362 In female sheep, the expression of mRNA involved with GSIS was altered in FGRS compared
363 to CON (SLC2A2 was increased and GCK was decreased), but was similar in FGRI compared
364 to CON (table 2); however, the expression of mRNA involved with mitochondria number and
365 function was increased in FGRS vs. CON (NRF1, UCP2, and MTATP6) and FGRI vs. CON
366 (TFAM and UCP2). mRNA expression was similar in FGRI and FGRS females, except SLC2A2
367 and NRF1, which was decreased, and TFAM, which was increased in FGRI compared to FGRS
368 females.

369

370 In contrast, SLC2A2, GCK, TFAM, NRF1, MTATP6, UCP2, and INS mRNA expression was
371 increased in FGRS compared to CON males. Conversely, in FGRI males, only the expression of
372 GCK was increased, and KCNJ11 and NRF1 expression was decreased compared to CON

males. There was decreased expression of most mRNA targets involved with GSIS and mitochondria, but not KCNJ11 and MTATP6, in FGRI compared to FGRS males (table 2).

Expression of mRNA involved with the maintenance of cell populations in whole pancreas.

In females, only IGF1 and FOXO1 mRNA expression was increased in FGRS compared to CON, with no differences in FGRI compared to CON (table 2). IGF1, INSR, and FOXO1 mRNA expression was decreased in FGRI compared to FGRS females.

In male sheep, both FGRS and FGRI had increased IGF2 expression and decreased IGFIR expression compared to CON. Male FGRS also had increased IGF1 expression compared to CON males. Overall, only IGF1 and IGF2 expression was decreased in FGRI compared to FGRS males (table 2).

Skeletal muscle insulin signaling pathway.

In female sheep, although there were some statistically significant differences in the expression of mRNA involved with the insulin signaling pathway amongst groups, the magnitude of the difference was small in all cases. In FGRS, AKT2 and PRKCZ expression was modestly decreased, and SLC2A2 expression was modestly increased compared to CON females. There were few changes in the mRNA expression in FGRI female skeletal muscle, with small increases in IRS1 and AKT2 compared to CON females, and in INSR and AKT2 compared to FGRS females (table 3).

In males, the mRNA expression of IRS1 and PRKCZ was decreased, and SLC2A4 expression was increased in FGRS compared to CON males. In contrast, IRS1, AKT2, PRKCZ, and SLC2A4 mRNA expression was decreased in FGRI compared to CON males. IRS1 and SLC2A4 mRNA expression were decreased, and AKT2 and PRKCZ expression were modestly increased in FGRI compared to FGRS males (table 3).

Expression of mitochondria number and function genes in skeletal muscle.

In females, the mRNA expression of all markers of mitochondria number and function in skeletal muscle were decreased in FGRS compared to CON (table 3). Only TFAM, UCP2, and GPX were decreased in FGRI compared to CON females. There were few changes in mRNA

405 expression between FGRI and FGRS, with NRF1 and GPX expression increased in FGRI
406 females (table 3).
407
408 Only the mRNA expression of NRF1, UCP2, and GPX were decreased in FGRS males
409 compared to CON males, with few changes measured in FGRI compared to CON males (table
410 3). PPARGC1A and MTATP6 mRNA expression were decreased, and UCP2 and GPX
411 expression were increased in FGRI compared to FGRS males (table 3).
412
413 In summary, we found that FGRI males demonstrated a ~225% increase in α-cell mass
414 compared to both CON and FGRS males. FGRS females and males, and FGRI females, but not
415 males, had increased expression of mitochondria-related mRNA expression in whole pancreas
416 samples compared to controls. FGRS females, FGRS males, and FGRI females demonstrated
417 decreased expression of mitochondria-related mRNA expression in skeletal muscle, but this
418 decrease was absent in FGRI males.
419

DISCUSSION

We have demonstrated that FGR and IGF-I therapy altered the cellular composition of the endocrine pancreas and the expression of mitochondria-related mRNA in both the pancreas and skeletal muscle in a sex-specific manner at 18-months of age.

In contrast to our hypothesis, we did not find differences in β-cell mass between groups in either sex. We hypothesized that FGR sheep would demonstrate decreased β-cell mass, postulating that this would contribute to the dampened insulin response throughout the ivGTT (33). In humans, decreased β-cell mass is associated with a reduced capacity to secrete insulin (13), and impaired insulin secretion following FGR becomes more pronounced with advancing age (44-47). In sheep, FGR fetuses near-term demonstrate reduced absolute β-cell mass followed by a compensatory increase in β-cell mass at one-month of age (11, 47). As we did not observe decreased β-cell mass in any group, it is likely that the decreased insulin response observed during ivGTT in growth-restricted female and male sheep indicates impaired β-cell function.

Interestingly, we found that α-cell mass was increased over two-fold exclusively in male FGRI sheep, with no change in other endocrine cell populations. One of the primary functions of glucagon, the predominant secretory product of α-cells, is to increase glucose secretion from the liver via glycogenolysis and gluconeogenesis in response to hypoglycemia (48). FGR is a major risk factor for neonatal hypoglycemia, yet little is known about the influence of the early life environment on α-cell mass and function. Previous studies of the effect of FGR on α-cell mass in the fetal and neonatal sheep are conflicting, with both reduced α-cell mass and no change being reported (35, 54-56), but we are not aware of any previous data in adults born FGR. α-cells also have other effects on pancreatic islet biology, including an essential role in the regulation of insulin secretion via paracrine signaling by glucagon (49). In lean, non-diabetic humans, α-cell mass and α-cell to β-cell mass ratios remain constant throughout adulthood (50), while individuals with T2DM demonstrate increased α-cell to β-cell mass ratios (51, 52). This is likely driven by β-cell loss rather than α-cell expansion (52), although there is evidence of trans-differentiation of α-cells into β-cells (53). We found no evidence that the increased α-cell to β-cell mass ratio was driven by β-cell loss in FGRI males, as β-cell mass was not different amongst groups. Aberrant glucagon secretion has been ascribed a pathophysiologic role in the progression of T2DM (48). In the early stages of the disease, glucagon may promote a compensatory increase in insulin output in individuals with impaired insulin secretion. As T2DM progresses, excessive

glucagon secretion can ultimately lead to diminished insulin stores, β-cell fatigue, and, eventually, β-cell apoptosis (13). As the increased α-cell mass observed in FGRI males was an unexpected finding, our study was not designed to interrogate the mechanistic causes of this change. Previous studies of IGF-I as a therapy for FGR did not assess endocrine cell populations in the pancreas. As we did not observe differences in insulin secretion in FGRI males, it is possible that increased α-cell mass was an adaptation to stimulate β-cells via paracrine mechanisms, to maintain insulin output. Due to the instability of glucagon in archival samples (57), we were not able to measure glucagon concentrations in plasma samples, nor were we able to measure intra-islet glucagon. Therefore, the function of the increased α-cell mass in FGRI males remains unclear; this novel finding should be the focus of future experiments.

FGR is associated with the downregulation of mRNA expression involved in mitochondrial function in isolated islets from fetal lambs (15). The ability of the β-cell to mount an insulin response is closely linked with mitochondrial function and glucose metabolism (58), with mitochondrial dysfunction frequently observed in β-cells of individuals with T2DM (59, 60). Impaired insulin secretion following FGR becomes more pronounced with advancing age (44-47). Surprisingly, we found increased expression of mRNA involved with mitochondrial function in whole-pancreas in FGRS compared with CON, in both sexes. However, fetal IGF-I therapy resulted in decreased expression of mitochondria-related mRNA in male, but not female, adult sheep. Decreased mRNA expression in FGRI males may indicate a predisposition to developing impaired mitochondrial function, and thus, impaired insulin secretion. However, given the relatively young age at which physiological testing and tissue collection were performed, and the heterogeneity of whole-pancreas tissue, it is unclear whether the adaptations measured would have led to physiological differences in insulin secretion with aging. Of note, whole pancreatic UCP2 mRNA expression was unchanged in FGRI males and was increased in FGRI females and FGRS sheep of both sexes compared to their respective CON groups. UCP2 negatively regulates the ability of the β-cell to secrete insulin, as UCP2 facilitates proton leak during oxidative phosphorylation, decreasing mitochondrial ATP output (61). Increased UCP2 expression is associated with β-cell dysfunction in isolated rodent islets (61, 62). Accordingly, increased UCP2 mRNA expression observed in FGRS sheep of both sexes, and in FGRI females may indicate impaired mitochondrial function, whilst the decreased UCP2 mRNA expression in FGRI males could be a compensatory mechanism to maintain ATP production and thus maintaining insulin secretion. Whether these changes in UCP2 expression negate the effects of altered mRNA expression of the other markers of mitochondrial function is unclear, and a functional

assessment of mitochondrial respiratory function would address this question. One limitation of our study is that we were unable to isolate pancreatic islets. To our knowledge, no one has yet successfully isolated islets from the pancreas of adult sheep. The expression of mitochondria-related mRNA targeted in this study are not specific to the endocrine pancreas. Therefore, we have measured mRNA expression of all resident cell populations and caution should be applied when interpreting the expression data.

We found that FGR and IGF-I therapy had a sex-specific effect on the expression of skeletal muscle mitochondria mRNA transcripts. All measured mRNA transcripts related to mitochondria number and function were decreased in female FGRS, but not FGRI, compared to CON. Whilst not statistically significant for all transcripts, a trend toward decreased expression remained in female FGRI compared to CON, to the point where with the exception of two transcripts, NRF1 and GPX, the expression of transcripts was similar between female FGRI and FGRS. Males, however, showed a different pattern of expression. Only half of the measured markers were decreased in FGRS compared to CON, and with the exception of MTATP6, there was no difference in expression of these mRNA transcripts between FGRI and CON males, suggesting that the effects of FGR on mitochondria are less in males and that IGF-I therapy mitigated the effects in females. Mitochondria are the primary site of ATP production in skeletal muscle and have a crucial role in maintaining metabolic homeostasis. Skeletal muscle mitochondrial dysfunction is common in individuals with insulin resistance (63, 64), and there is increasing evidence that this dysfunction is found in individuals with FGR (65). Given that IGF-I therapy had limited effects on the expression of mitochondria-related mRNA in female sheep, this treatment may ameliorate the negative effects of FGR in males only. Given the effect of IGF-I therapy on the expression of mitochondria-related mRNA in both whole pancreas and skeletal muscle, assessment of mitochondrial respiratory function following this treatment would be a novel avenue to explore.

Finally, we found decreased skeletal muscle mRNA expression of transcripts associated with insulin signaling in male FGRS and FGRI sheep compared to controls. Humans who experienced FGR have a predisposition to developing insulin resistance later in life (8, 9, 66), which is often accompanied by decreased INSR, IRS1, AKT2, PRKCZ, and SLC2A4 mRNA expression in skeletal muscle in both humans and sheep models of FGR (19-23). Furthermore, decreased expression of these components is frequently reported in individuals with insulin resistance (24, 67, 68). Therefore, although insulin sensitivity was not different between groups at

18-months of age, the decreased pattern of expression of mRNA transcripts associated with the insulin signaling pathway may indicate that these sheep are predisposed to the subsequent development of skeletal muscle insulin resistance. Future studies should investigate the effect of IGF-I treatment of the FGR fetus at a more advanced age, as it is likely that 18-months was too young for an overt phenotype to develop in this model.

Strengths and limitations.

This is the first study to demonstrate that IGF-I therapy of the FGR fetus has long-term effects on metabolically active tissues in adult sheep. Specifically, we found alterations in the cellular composition of the endocrine pancreas and the expression of metabolically-associated mRNA transcripts in the whole pancreas and skeletal muscle. Importantly, this study was powered to detect sex-specific changes in physiologic measurements and adds to the growing body of evidence that supports the use of both sexes in preclinical research on treatments for FGR. However, we acknowledge several limitations. First, it is possible that the detrimental effects of FGR and any beneficial effects of IGF-I therapy were subtle at 18-months of age compared to what may occur with increased age. The lifespan of domesticated sheep is estimated to be 12-14 years for females and 10-12 years for males (69). In human studies, overt T2DM in individuals with FGR is generally evident in adults aged over 50-years (8, 66). Therefore, 18-months of age may have been too young to detect an overt phenotype. We explored two key metabolically active tissues: the endocrine pancreas and skeletal muscle. Other tissues, such as adipose tissue, the liver, and the brain, contribute to maintaining glucose homeostasis. Exploring these tissues would provide a more holistic image of the effect of IGF-I therapy but were beyond the scope of the current study. Moreover, the samples in our study were collected from animals that were fasted at tissue collection. There is evidence that insulin resistance is mediated via dampened activation of the insulin signaling pathway, such as Akt activation state or SLC2A4 translocation (70). A muscle biopsy immediately after HGC should be taken to assess the direct effect of insulin stimulation on skeletal muscle. Finally, these studies were performed as a secondary analysis of tissues collected as part of a larger study, which was designed to investigate the effect of IGF-I therapy on physiologic outcomes at 18-months of age. Therefore, it was not possible to further interrogate the relationships between our unexpected findings and the physiology of these sheep following IGF-I therapy and increased α-cell mass in FGRI males, or whether altered expression of mitochondria-related mRNA impart a functional effect on pancreatic or skeletal muscle mitochondria. Future research into IGF-I treatment of FGR should further interrogate the mechanistic implications of these novel findings.

CONCLUSION

This study demonstrates that IGF-I therapy of FGR altered the endocrine pancreas and skeletal muscle in a sex-specific manner independent of insulin secretion or insulin sensitivity in sheep at 18 months of age. Despite the brief IGF-I treatment window, changes at the tissue and cellular levels persisted to young adulthood. Future studies should specifically explore whether this therapy impacts mitochondrial function in both the endocrine pancreas and skeletal muscle, and the functional consequences of increased α-cell mass in IGF-I treated males. Given that a metabolic phenotype is likely to develop as FGR sheep reach mid-to-late adulthood, it remains unclear whether IGF-I therapy-mediated adaptations would ameliorate or worsen the development of FGR-associated metabolic disease.

Since individuals with FGR are predisposed to develop impaired insulin secretion and insulin resistance in adulthood, it is clear that early life interventions which aim to both improve neonatal outcomes and ameliorate the risk of developing metabolic disease must be developed. Therefore IGF-I therapy warrants further investigation.

REFERENCES

1. **Nardozza LMM, Caetano ACR, Zamarian ACP, Mazzola JB, Silva CP, Marcal VMG, Lobo TF, Peixoto AB, and Junior EA**. Fetal growth restriction: current knowledge. *Archives of Gynecology and Obstetrics* 295: 1061-1077, 2017.

2. **Bernstein IM, Horbar JD, Badger GJ, Ohlsson A, and Golan A**. Morbidity and mortality among very-low-birth-weight neonates with intrauterine growth restriction. *American Journal of Obstetrics & Gynecology* 182: 198-206, 2000.

3. **Gilbert WM, and Danielsen B**. Pregnancy outcomes associated with intrauterine growth restriction. *American Journal of Obstetrics & Gynecology* 188: 1596-1601, 2003.

4. **Garite TJ, Clark R, and Thorp JA**. Intrauterine growth restriction increases morbidity and mortality among premature neonates. *American Journal of Obstetrics & Gynecology* 191: 481-487, 2004.

5. **Figueras F, Caradeux J, Crispi F, Eixarch E, Peguero A, and Gratacos E**. Diagnosis and surveillance of late-onset fetal growth restriction. *American Journal of Obstetrics & Gynecology* 218: S790-S802, 2018.

6. **Resnik R**. Intrauterine growth restriction. *Obstetrics & Gynecology* 99: 490-496, 2002.

7. **Groom KM, and David AL**. The role of aspirin, heparin, and other interventions in the prevention and treatment of fetal growth restriction. *American Journal of Obstetrics & Gynecology* 218: S829-S840, 2018.

8. **Hales CN, Barker DJP, Clark PMS, Cox LJ, Fall C, Osmond C, and Winter PD**. Fetal and infant growth and impaired glucose tolerance at age 64. *British Medical Journal* 303: 1019-1022, 1991.

9. **Barker DJP**. Adult consequences of fetal growth restriction. *Clinical Obstetrics and Gynecology* 49: 270-283, 2006.

10. **Warner MJ, and Ozanne SE**. Mechanisms involved in the developmental programming of adulthood disease. *Biochemical Journal* 427: 333-347, 2010.

11. **Boehmer BH, Limesand SW, and Rozance PJ**. The impact of IUGR on pancreatic islet development and β-cell function. *Journal of Endocrinology* 235: R63-R76, 2017.

12. **Bouwens L, and Rooman I**. Regulation of pancreatic beta-cell mass. *Physiological Reviews* 85: 1255-1270, 2005.

13. **Weir GC, and Bonner-Weir S**. Islet β cell mass in diabetes and how it relates to function, birth, and death. *Annals of the New York Academy of Sciences* 1281: 92-105, 2013.

14. **Limesand SW, Rozance PJ, Zerbe GO, Hutton JC, and Hay Jr WW**. Attenuated insulin release and storage in fetal sheep pancreatic islets with intrauterine growth restriction. *Endocrinology* 147: 1488-1497, 2006.

15. **Kelly AC, Bidwell CA, McCarthy FM, Taska DJ, Anderson MJ, Camacho LE, and Limesand SW**. RNA sequencing exposes adaptive and immune responses to intrauterine growth restriction in fetal sheep islets. *Endocrinology* 158: 743-755, 2017.

16. **Brown LD, and Hay WW**. Impact of placental insufficiency on fetal skeletal muscle growth. *Molecular and Cellular Endocrinology* 432: 69-77, 2016.

17. **Zhu MJ, Ford SP, Means WJ, Hess BW, Nathanielsz PW, and Du M**. Maternal nutrient restriction affects properties of skeletal muscle in offspring. *Journal of Physiology* 575: 241-250, 2006.

18. **Yliharsila H, Kajantie E, Osmond C, Forsen T, Barker DJP, and Eriksson JG**. Birth size, adult body composition and muscle strength in later life. *International Journal of Obesity* 31: 1392-1399, 2007.

19. **De Blasio MJ, Gatford KL, Harland ML, Robinson JS, and Owens JA**. Placental restriction reduces insulin sensitivity and expression of insulin signaling and glucose transporter genes in skeletal muscle, but not liver, in young sheep. *Endocrinology* 153: 2142-2151, 2012.

20. **Thorn SR, Regnault TRH, Brown LD, Rozance PJ, Keng J, Roper M, Wilkening RB, Hay WW, Jr., and Friedman JE**. Intrauterine growth restriction increases fetal hepatic gluconeogenic capacity and reduces messenger ribonucleic acid translation initiation and nutrient sensing in fetal liver and skeletal muscle. *Endocrinology* 150: 3021-3030, 2009.

21. **Ozanne SE, Jensen CB, Tingey KJ, Storgaard H, Madsbad S, and Vaag A**. Low birthweight is associated with specific changes in muscle insulin-signalling protein expression. *Diabetologia* 48: 547-552, 2005.

22. **Jensen CB, Martin-Gronert MS, Storgaard H, Madsbad S, Vaag A, and Ozanne SE**. Altered PI3-kinase/Akt signalling in skeletal muscle of young men with low birth weight. *PLoS ONE* 3: e3738, 2008.

23. **Muhlhausler BS, Duffield JA, Ozanne SE, Pilgrim C, Turner N, Morrison JL, and McMillen IC**. The transition from fetal growth restriction to accelerated postnatal growth: a potential role for insulin signalling in skeletal muscle. *Journal of Physiology* 587: 4199-4211, 2009.

24. **Samuel VT, and Shulman GI**. The pathogenesis of insulin resistance: integrating signaling pathways and substrate flux. *The Journal of Clinical Investigation* 126: 12-22, 2016.

25. **Aiken CE, and Ozanne SE**. Sex differences in developmental programming models. *Reproduction* 145: R1-R13, 2013.

26. **Dearden L, Bouret SG, and Ozanne SE**. Sex and gender differences in developmental programming of metabolism. *Molecular Metabolism* 15: 8-19, 2018.

27. **Wali JA, de Boo HA, Derraik JGB, Phua HH, Oliver MH, Bloomfield FH, and Harding JE**. Weekly intra-amniotic IGF-I treatment increases growth of growth-restricted ovine fetuses and up-regulates placental amino acid transporters. *PLoS ONE* 7: e37899, 2012.

28. **Eremia SC, de Boo HA, Bloomfield FH, Oliver MH, and Harding JE**. Fetal and amniotic insulin-like growth factor-I supplements improve growth rate in intrauterine growth restriction in fetal sheep. *Endocrinology* 148: 2963-2972, 2007.

29. **Spiroski A-M, Oliver MH, Jaquiery AL, Prickett TCR, Espiner EA, Harding JE, and Bloomfield FH**. Postnatal effects of intrauterine treatment of the growth-restricted ovine fetus with intra-amniotic insulin-like growth factor-1. *Journal of Physiology* 596: 5925-5945, 2017.

30. **Darp RA, de Boo HA, Phua HH, Oliver MH, Derraik JGB, Harding JE, and Bloomfield FH**. Differential regulation of igf1 and igf1r mRNA levels in the two hepatic lobes following intrauterine growth restriction and its treatment with intra-amniotic insulin-like growth factor-1 in ovine fetuses. *Reproduction, Fertility and Development* 22: 1188-1197, 2010.

31. **Bloomfield FH, Bauer MK, Van Zijl PL, Gluckman PD, and Harding JE**. Amniotic IGF-I supplements improve gut growth but reduce circulating IGF-I in growth-restricted fetal sheep. *American Journal of Physiology - Endocrinology and Metabolism* 282: E259-E269, 2002.

32. **Bloomfield FH, van Zijl PL, Bauer MK, and Harding JE**. Effects of intrauterine growth restriction and intraamniotic insulin-like growth factor-I treatment on blood and amniotic fluid concentrations and on fetal gut uptake of amino acids in late-gestation ovine fetuses. *Journal of Pediatric Gastroenterology and Nutrition* 35: 287-297, 2002.

33. **Spiroski A-M, Oliver MH, Jaquiery AL, Gunn TD, Harding JE, and Bloomfield FH**. Effects of intrauterine insulin-like growth factor-1 therapy for fetal growth restriction on adult metabolism and body composition are sex specific. *American Journal of Physiology - Endocrinology and Metabolism* 318: E568-E578, 2020.

34. **Kilkenny C, Browne W, Cuthill IC, Emerson M, and Altman DG**. Animal research: reporting in vivo experiments: the ARRIVE guidelines. *British Journal of Pharmacology* 160: 1577-1579, 2010.

35. **Limesand SW, Jensen J, Hutton JC, and Hay WW**. Diminished β-cell replication contributes to reduced β-cell mass in fetal sheep with intrauterine growth restriction. *American Journal of Physiology - Regulatory, Integrative and Comparative Physiology* 288: R1297-R1305, 2005.

36. **Leos RA, Anderson MJ, Chen X, Pugmire J, Anderson KA, and Limesand SW**. Chronic exposure to elevated norepinephrine suppresses insulin secretion in fetal sheep with placental insufficiency and intrauterine growth restriction. *American Journal of Physiology - Endocrinology and Metabolism* 298: E770-E778, 2010.

37. **Cole L, Anderson M, Antin PB, and Limesand SW**. One process for pancreatic β-cell coalescence into islets involves an epithelial-mesenchymal transition. *Journal of Endocrinology* 203: 19-31, 2009.

38. **Schindelin J, Arganda-Carreras I, Frise E, Kaynig V, Longair M, Pietzsch T, Preibish S, Rueden C, Saalfeld S, Schmid B, Tinevez J-Y, White DJ, Hartenstein V, Eliceiri K, Tomancak P, and Cardona A**. Fiji: an open-source platform for biological-image analysis. *Nature Methods* 9: 676-682, 2012.

39. **Brereton MF, Vergari E, Zhang Q, and Clark A**. Alpha-, delta-, and PP-cells: are they the architectural cornerstones of islet structure and co-ordination? *Journal of Histochemistry & Cytochemistry* 63: 575-591, 2015.

40. **Antonov J, Goldstein DR, Oberli A, Baltzer A, Pirotta M, Fleischmann A, Altermatt HJ, and Jaggi R**. Reliable gene expression measurements from degraded RNA by

688 quantitative real-time PCR depend on short amplicons and a proper normalization. *Laboratory*
689 *Investigation* 85: 1040-1050, 2005.

690 41. **Fleige S, and Pfaffl MW**. RNA integrity and the effect on the real-time qRT-PCR
691 performance. *Molecular Aspects of Medicine* 27: 126-139, 2006.

692 42. **Altschul SF, Gish W, Miller W, Myers EW, and Lipman DJ**. Basic local alignment
693 search tool. *Journal of Molecular Biology* 215: 403-410, 1990.

694 43. **Pfaffl MW**. A new mathematical model for relative quantification in real-time RT-PCR.
695 *Nucleic Acids Research* 29: 2002-2007, 2001.

696 44. **Mericq V, Ong KK, Bazaes R, Pena V, Avila A, Salazar T, Soto N, Iniguez G, and**
697 **Dunger D**. Longitudinal changes in insulin sensitivity and secretion from birth to age three years
698 in small- and appropriate-for-gestational-age children. *Diabetologia* 48: 2609-2614, 2005.

699 45. **Veening MA, Van Weissenbruch MM, Heine RJ, and Delemarre-Van de Waal**
700 **HA**. β-cell capacity and insulin sensitivity in prepubertal children born small for gestational age:
701 influence of body size during childhood. *Diabetes* 52: 1756-1760, 2003.

702 46. **Jensen CB, Storgaard H, Dela F, Holst JJ, Madsbad S, and Vaag AA**. Early
703 differential defects of insulin secretion and action in 19-year-old caucasian men who had low
704 birth weight. *Diabetes* 51: 1271-1280, 2002.

705 47. **Gatford KL, and Simmons RA**. Prenatal programming of insulin secretion in
706 intrauterine growth restriction. *Clinical Obstetrics and Gynecology* 56: 520-528, 2013.

707 48. **Ahren B**. Glucagon - early breakthroughs and recent discoveries. *Peptides* 67: 74-81, 2015.

708 49. **Rodriguez-Diaz R, Tamayo A, Hara M, and Caicedo A**. The local paracrine actions
709 of the pancreatic α-cell. *Diabetes* 69: 550-558, 2020.

710 50. **Moin ASM, Cory M, Gurlo T, Sisho Y, Rizza RA, Butler PC, and Butler AE**.
711 Pancreatic alpha-cell mass across adult human lifespan. *European Journal of Endocrinology* 182: 219-
712 231, 2020.

713 51. **Fujita Y, Kozawa J, Iwahashi H, Yoneda S, Uno S, Eguchi H, Nagano H,**
714 **Imagawa A, and Shimomura I**. Human pancreatic α- to β-cell area ratio increases after type 2
715 diabetes onset. *Journal of Diabetes Investigation* 9: 1270-1282, 2018.

716 52. **Kilimnik G, Zhao B, Jo J, Periwal V, Witkowski P, Misawa R, and Manami H**.
717 Altered islet composition and disproportionate loss of large islets in patients with type 2 diabetes.
718 *PLoS ONE* 6: e27445, 2011.

719 53. **Habener JF, and Stanojevic V**. Alpha cells come of age. *TRENDS in Endocrinology and*
720 *Metabolism* 24: 153-163, 2013.

721 54. **Limesand SW, Rozance PJ, Macko AR, Anderson MJ, Kelly AC, and Hay WW**.
722 Reductions in insulin concentrations and β-cell mass precede growth restrictions in sheep fetuses
723 with placental insufficiency. *American Journal of Physiology - Endocrinology and Metabolism* 304: E516-
724 E523, 2013.

55. **Davis MA, Macko AR, Steyn LV, Anderson MJ, and Limesand SW**. Fetal adrenal demedullation lowers circulating norepinephrine and attenuates growth restriction but not reduction of endocrine cell mass in an ovine model of intrauterine growth restriction. *Nutrients* 7: 500-516, 2015.

56. **Camacho LE, Chen X, Hay Jr WW, and Limesand SW**. Enhanced insulin secretion and insulin sensitivity in young lambs with placental insufficiency-induced intrauterine growth restriction. *Am J Physiol Regul Integr Comp Physiol* 313: R101-R109, 2017.

57. **Cegla J, Jones BJ, Howard J, Kay R, Creaser CS, Bloom SR, and Tan TM**. The preanalytical stability of glucagon as measured by liquid chromatography tandem mass spectrometry and two commercially available immunoassays. *Annals of Clinical Biochemistry* 54: 293-296, 2017.

58. **Henquin J-C**. Triggering and amplifying pathways of regulation of insulin secretion by glucose. *Diabetes* 49: 1751-1760, 2000.

59. **Robertson RJ, Harmon J, Tran POT, and Poitout V**. β-cell glucose toxicity, lipotoxicity, and chronic oxidative stress in type 2 diabetes. *Diabetes* 53: S119-S124, 2004.

60. **Maechler P, and Wollheim CB**. Mitochondrial function in normal and diabetic β-cells. *Nature* 414: 807-812, 2001.

61. **Zhang C-Y, Baffy G, Perret P, Krauss S, Peroni O, Grujic D, Hagen T, Vidal-Puig AJ, Boss O, Kim Y-B, Zheng XX, Wheeler MB, Shulman GI, Chan CB, and Lowell BB**. Uncoupling protein-2 negatively regulates insulin secretion and is a major link between obesity, β cell dysfunction, and type 2 diabetes. *Cell* 105: 745-755, 2001.

62. **de Souza BM, Assmann TS, Kliemann LM, Gross JL, Canani LH, and Crispim D**. The role of uncoupling protein 2 (UCP2) on the development of type 2 diabetes mellitus and its chronic complications. *Arquivos Brasileiros de Endocrinologia & Metabologia* 55: 239-248, 2011.

63. **Rovira-Llopis S, Banuls C, Diaz-Morales N, Hernandez-Mijares A, Rocha M, and Victor VM**. Mitochindrial dynamics in type 2 diabetes: pathophysiological implications. *Redox Biology* 11: 637-645, 2017.

64. **Crescenzo R, Bianco F, Mazzoli A, Giacco A, Liverini G, and Iossa S**. Mitochondrial efficiency and insulin resistance. *Frontiers in Physiology* 5: 512, 2015.

65. **Gyllenhammer LE, Entringer S, Buss C, and Wadhwa PD**. Developmental programming of mitochondrial biology: a conceptual framework and review. *Proceedings of the Royal Society B* 287: 1926, 2020.

66. **Barker DJP, Hales CN, Fall CHD, Osmond C, Phipps K, and Clark PMS**. Type 2 (non-insulin-dependent) diabetes mellitus, hypertension, and hyperlipidaemia (syndrome X): relation to reduced fetal growth. *Diabetologia* 36: 62-67, 1993.

67. **Sreekumar R, Halvatsiotis P, Schimke JC, and Nair KS**. Gene expression profile in skeletal muscle of type 2 diabetes and the effect of insulin treatment. *Diabetes* 51: 1913-1920, 2002.

763 68. **Elbein SC, Kern PA, Rasouli N, Yao-Borengasser A, Sharma NK, and Das SK**.
764 Global gene expression profiles of subcutaneous adipose and muscle from glucose-tolerant,
765 insulin-sensitive, and insulin-resistant indivudals matched for BMI. *Diabetes* 60: 1019-1029, 2011.

766 69. **Osterman SD, Deforge JR, and Edge WD**. Captive breeding and reintroduction
767 evaluation criteria: a case study of peninsular bighorn sheep. *Conservation Biology* 15: 749-760,
768 2001.

769 70. **Sylow L, Kleinert M, Pehmoller C, Prats C, Chiu TT, Klip A, Richter EA, and**
770 **Jensen TE**. Akt and Rac1 signaling are jointly required for insulin-stimulated glucose uptake in
771 skeletal muscle and downregulated in insulin resistance. *Cellular Signalling* 26: 323-331, 2014.
772
773

ACKNOWLEDGEMENTS

The authors thank Marcus Ground for assistance with drawing figures 1A, 1B, and the graphical abstract.

FIGURE LEGENDS

Figure 1.

Overview of the glucose-stimulated insulin secretion (GSIS) pathway (A) and the insulin signaling pathway in skeletal muscle (B).

During GSIS (A), glucose is transported into the β-cell via solute carrier family 2 member 2 (SLC2A2) transporters, where it is phosphorylated by glucokinase (GCK) into glucose 6-phosphate. Glucose 6-phosphate is metabolised via oxidative phosphorylation in mitochondria increasing the intracellular ATP:ADP ratio. This induces ATP-sensitive potassium channels to close, increasing intracellular potassium concentration, and leading to membrane depolarisation. In turn, calcium channels are opened, promoting the exocytosis of insulin granules at the surface of the β-cell into the circulation. A bold font indicates rate-limiting processes. Gene names in boxes next to each process indicate mRNA expression measured in the current study; genes associated with promoting or inhibiting these processes have been indicated with green or blue boxes, respectively. Gene names (gene symbol): solute carrier family 2 member 2 (SLC2A2); glucokinase (GCK); potassium voltage-gated channel subfamily J member 11 (KCNJ11); transcription factor A (TFAM); nuclear respiratory factor 1 (NRF1); uncoupling protein 2 (UCP2); mitochondrially encoded ATP synthase membrane subunit 6 (MTATP6); insulin (INS).

During insulin signaling in skeletal muscle (B), insulin binds to the insulin receptor (IR), which is autophosphorylated and, in turn, phosphorylates insulin receptor substrate (IRS)-1. IRS-1 activates phosphatidylinositol 3-kinase (PI3K), which catalyses the generation of the secondary signaling molecule phosphatidylinositol (3,4,5)-triphosphate (PIP_3) from phosphatidylinositol (4,5)-bisphosphate (PIP_2). PIP_3 subsequently recruits downstream signaling proteins, including protein kinase C (PKC) and 3-phosphoinositide-dependent protein kinase 1 (PDK1); PDK1 activates Akt2, which is responsible for many of the metabolic actions of insulin, including AS160. PKCζ and AS160 are responsible for the transportation of SLC2A4 to the cell surface, allowing increased glucose transport into the cell. Gene names in boxes next to each process indicate mRNA expression measured in the current study; genes associated with promoting or

inhibiting these processes have been indicated with green or blue boxes, respectively. Gene names (gene symbol): insulin receptor, β-subunit (INSR); insulin receptor substrate 1 (IRS1); phosphatidylinositol-4,5-bisphosphate 3-kinase catalytic subunit beta (PIK3CB); AKT serine/threonine kinase 2 (AKT2); protein kinase c zeta (PRKCZ); solute carrier family 2 member 4 (SLC2A4); peroxisome proliferator activated receptor gamma coactivator 1 Alpha (PPARGC1A); transcription factor A (TFAM); nuclear respiratory factor 1 (NRF1); uncoupling protein 2 (UCP2); mitochondrially encoded ATP synthase membrane subunit 6 (MTATP6). Created with BioRender.com.

Figure 2.

Representative composite immunofluorescent staining images for endocrine cell populations in lamb pancreas at 18-months of age in female and male CON (A-B), FGRS (C-D), and FGRI (E-F) lambs. Each composite image is composed of immunofluorescence staining against insulin (red), glucagon (green), somatostatin (yellow), and nuclei (blue), to identify pancreatic endocrine cell types β, α, and δ, respectively. Scale bars represent 100 μm.

Figure 3.

Scatter plots of β-cell mass vs. plasma and insulin responses to ivGTT in female (A) CON (white, n=7), FGRS (grey, n=7), and IGFI (black, n=7) and male (B) CON (white, n=7), FGRS (grey, n=7), and IGFI (black, n=8) sheep at 18-months of age.

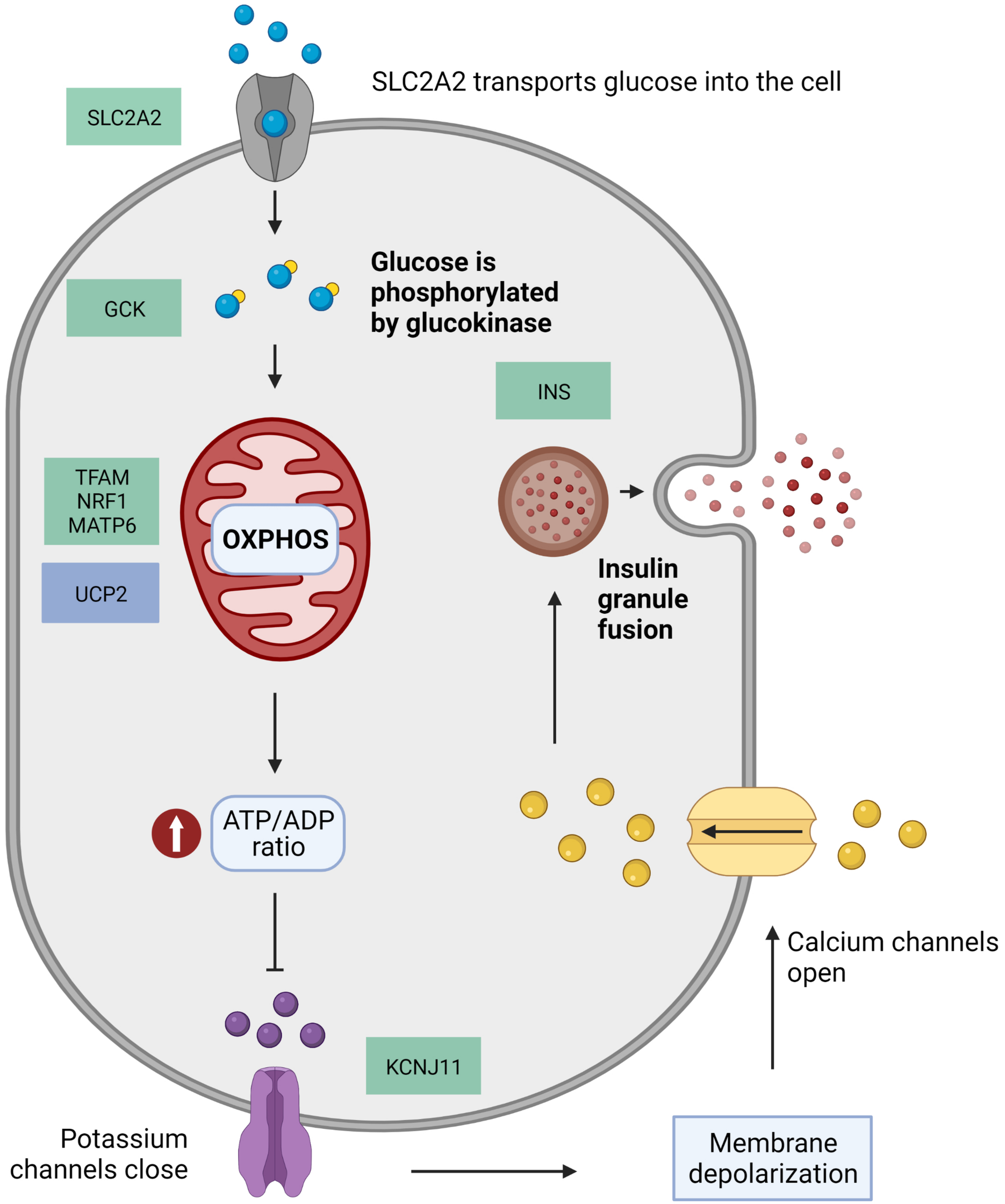

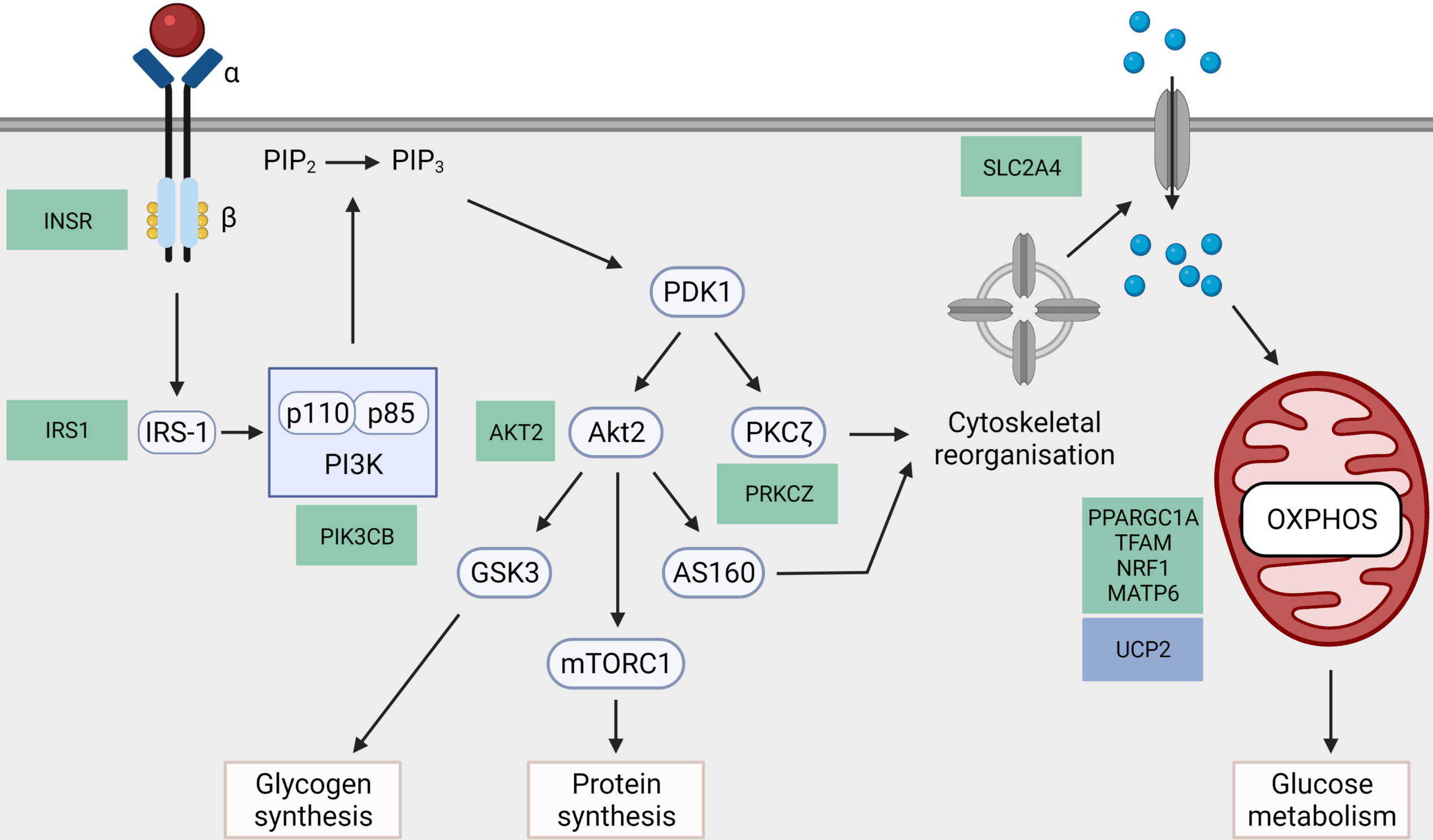

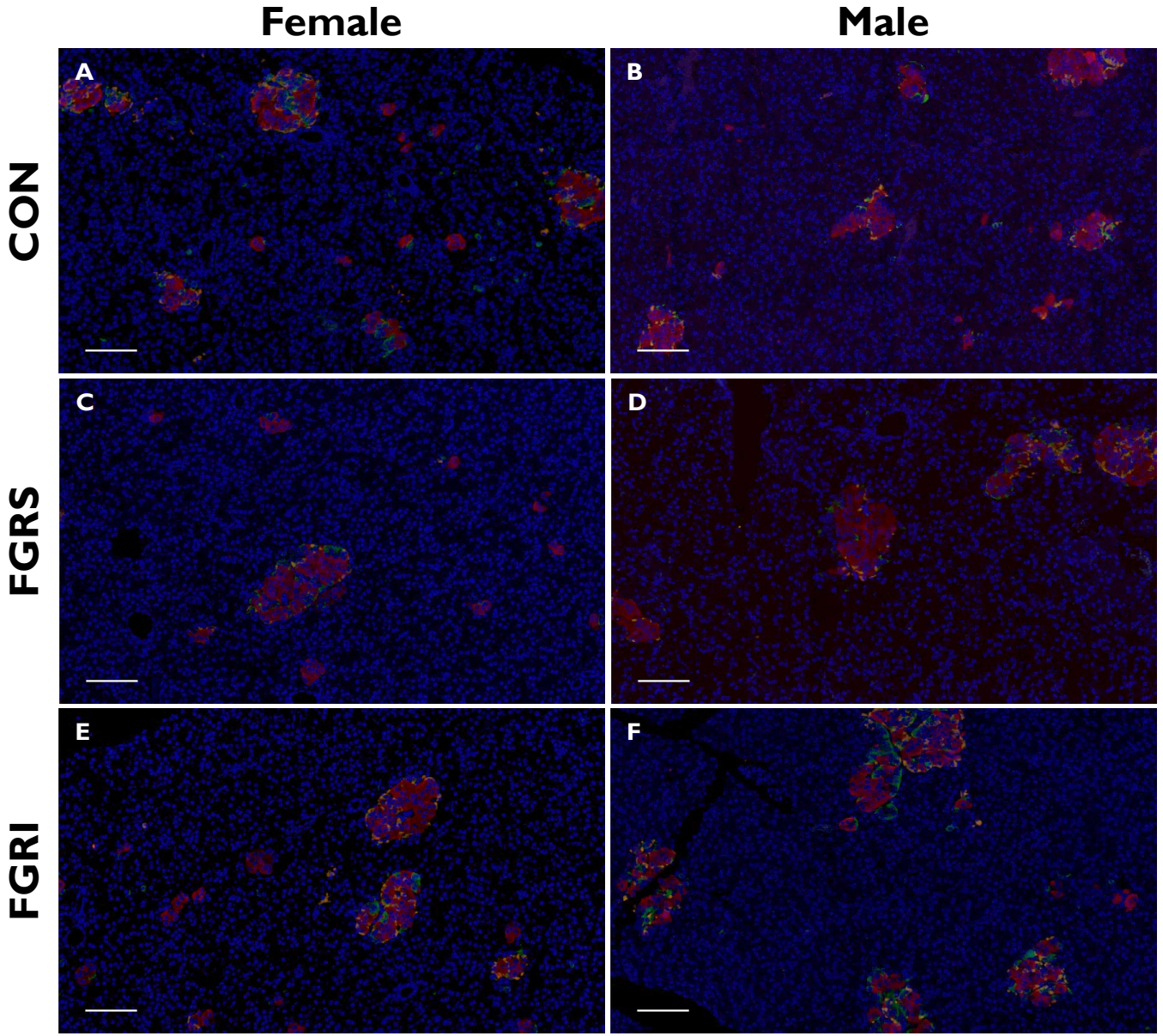

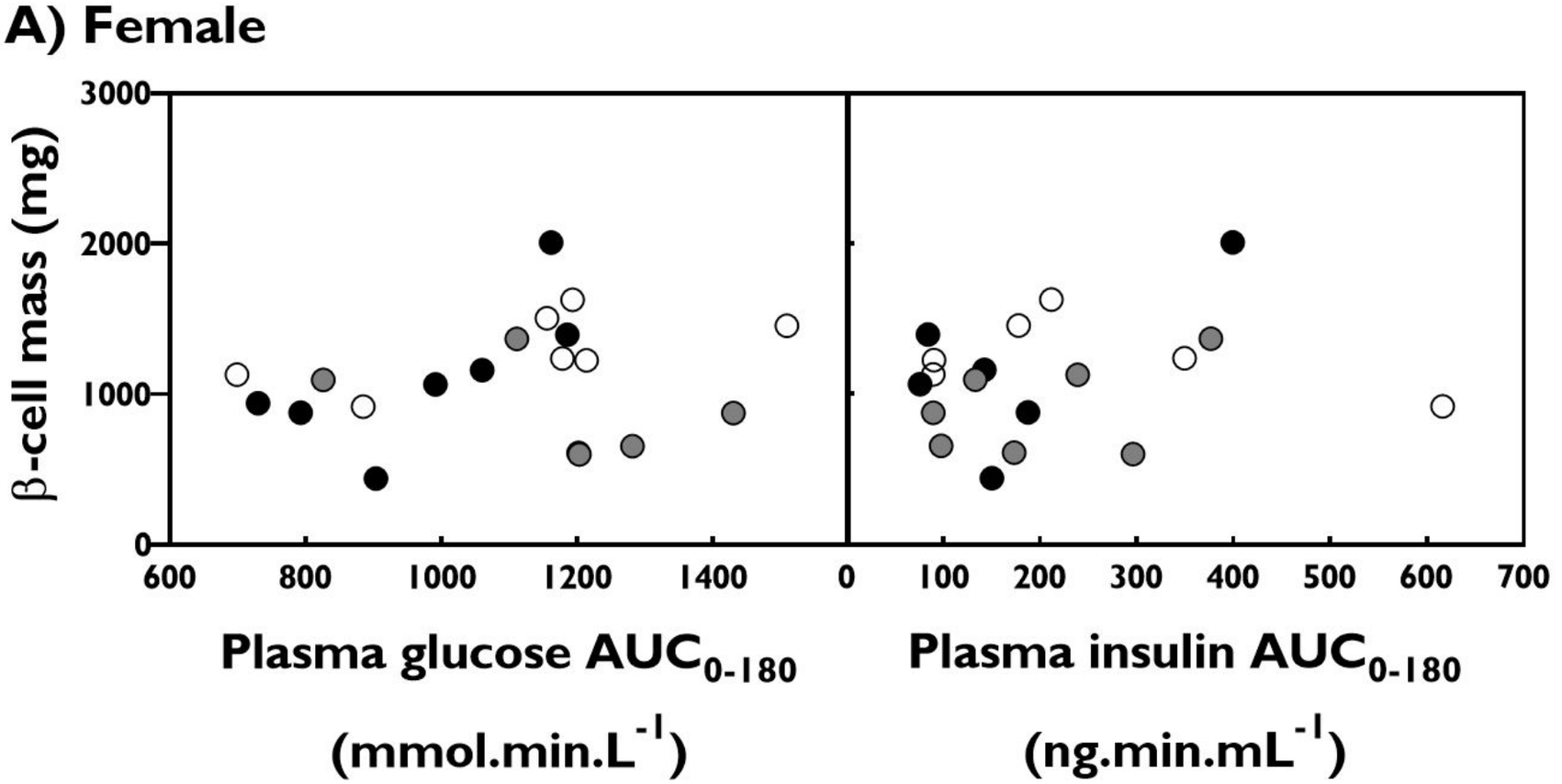

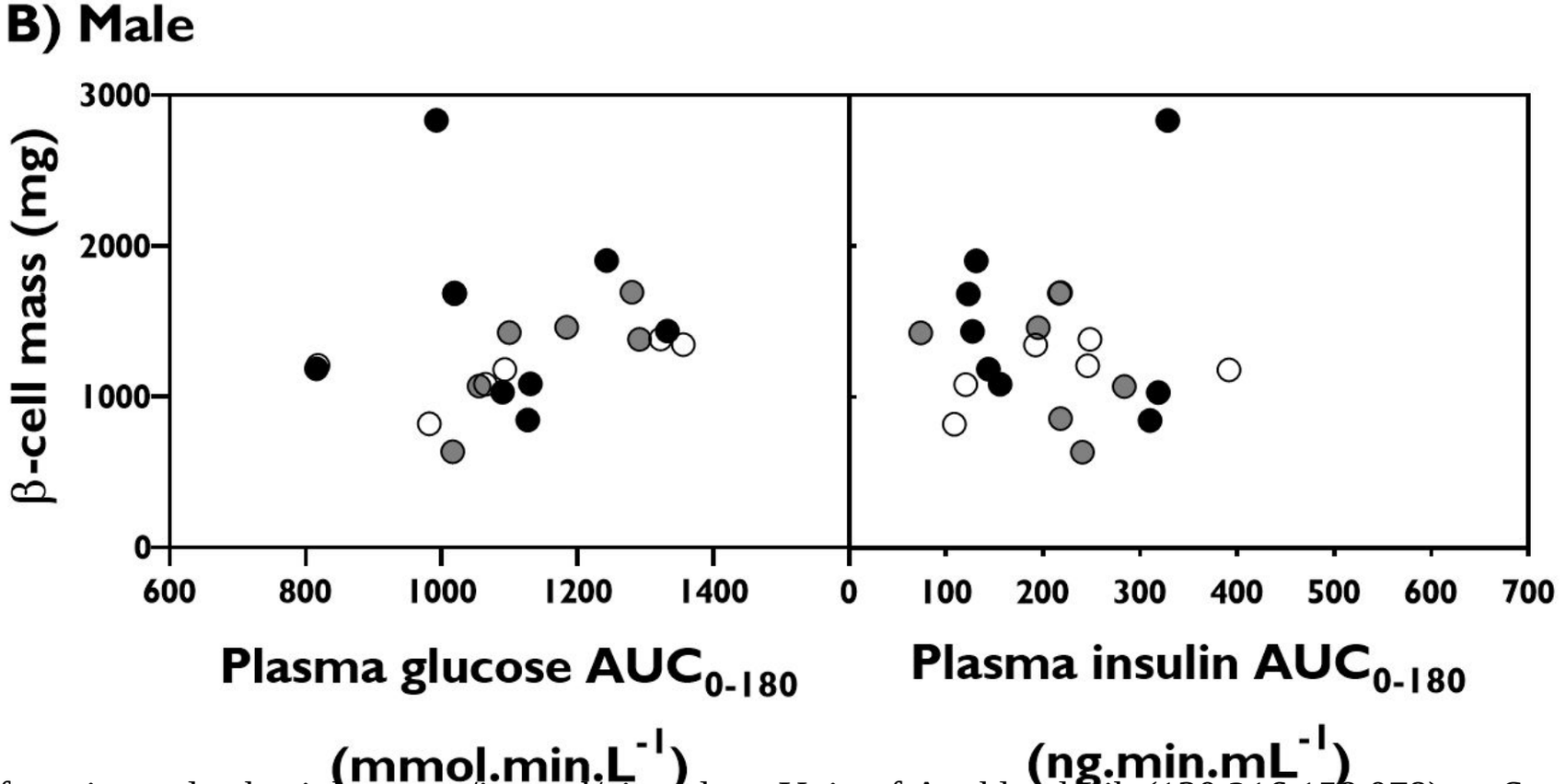

Table 1.

Endocrine pancreas cell populations at 18-months of age.

	Female			Male			p value (treatment effect)	
	CON n=7	FGRS n=7	FGRI n=7	CON n=7	FGRS n=7	FGRI n=8	Female	Male
Tissue measured (mm^2)	136 ± 15	128 ± 12	119 ± 16	108 ± 11	115 ± 14	92 ± 10	N/A	N/A
Absolute endocrine cell mass								
Total islet cell mass (mg)	1492 ± 92	1028 ± 118	1395 ± 211	1529 ± 132	1427 ± 170	1802 ± 265	ns	ns
β-cell mass (mg)	1301 ± 92	906 ± 114	1127 ± 184	1245 ± 102	1218 ± 142	1501 ± 227	ns	ns
α-cell mass (mg)	48 ± 12	33 ± 3	48 ± 10	53 ± 14[a]	54 ± 10[a]	120 ± 18[b]	ns	0.005
δ-cell mass (mg)	143 ± 26[ab]	89 ± 13[ac]	219 ± 33[b]	231 ± 38	155 ± 42	182 ± 37	0.006	ns
Ratio of α:β cell mass	0.037 ± 0.01	0.040 ± 0.01	0.043 ± 0.01	0.040 ± 0.01[a]	0.046 ± 0.01[a]	0.081 ± 0.01[b]	ns	0.001
Endocrine cell mass relative to total islet cell mass								
Relative β-cell mass (%)	87.0 ± 1.7	87.5 ± 1.6	80.9 ± 2.3	81.7 ± 2.2	85.7 ± 2.1	83.2 ± 1.3	0.045	ns
Relative α-cell mass (%)	3.2 ± 0.7	3.5 ± 0.4	3.3 ± 0.6	3.3 ± 0.6[a]	3.9 ± 0.6[a]	6.7 ± 0.6[b]	ns	0.008
Relative δ-cell mass (%)	9.8 ± 1.8[a]	9.1 ± 1.3[a]	15.8 ± 1.8[b]	15.0 ± 2.1	10.4 ± 2.1	10.1 ± 1.5	0.020	ns
Endocrine cell mass relative to bodyweight at tissue collection								
Relative β-cell mass $\times 10^{-5}$ (%)	164 ± 12	116 ± 14	156 ± 21	142 ± 15	140 ± 17	169 ± 24	0.100	ns
Relative α-cell mass $\times 10^{-5}$ (%)	5.9 ± 1.5	4.3 ± 0.3	6.8 ± 1.4	6.2 ± 1.7[a]	6.2 ± 1.0[a]	13.4 ± 1.9[b]	ns	0.006
Relative δ-cell mass$\times 10^{-5}$ (%)	18.6 ± 3.6[ab]	11.6 ± 1.9[a]	30.9 ± 4.6[bc]	26.9 ± 4.9	19.0 ± 5.8	20.8 ± 4.3	0.004	ns

Data are means ± SEM. Relative endocrine cell masses are expressed relative to total islet cell mass or relative to bodyweight at tissue collection. For each sex, data were compared using 1-way ANOVA with treatment as a factor. Means with different letters indicate $p<0.05$ following Tukey post hoc testing.

Table 2.

Whole pancreas gene expression at 18-months of age.

	Female			Male		
Gene symbol	FGRS vs. CON	FGRI vs. CON	FGRI vs. FGRS	FGRS vs. CON	FGRI vs. CON	FGRI vs. FGRS
GSIS						
SLC2A2#	1.25 (1.22, 1.29)*	0.90 (0.72, 1.13)	0.72 (0.60, 0.87)*	1.39 (1.33, 1.45)*	1.17 (0.95, 1.45)	0.83 (0.73, 0.94)*
GCK#	0.81 (0.72, 0.91)*	0.93 (0.77, 1.13)	1.15 (0.94, 1.39)	1.30 (1.14, 1.47)*	1.14 (1.00, 1.29)*	0.88 (0.82, 0.94)*
KCNJ11#	1.11 (0.84, 1.46)	1.23 (0.90, 1.68)	1.11 (0.90, 1.37)	0.91 (0.83, 1.01)	0.84 (0.81, 0.87)*	0.92 (0.81, 1.05)
Mitochondria number and function						
TFAM	1.02 (0.78, 1.35)	1.40 (1.24, 1.58)*	1.37 (1.21, 1.54)*	1.40 (1.01, 1.93)*	0.94 (0.76, 1.15)	0.67 (0.51, 0.89)*
NRF1	1.56 (1.07, 2.27)*	1.12 (0.96, 1.31)	0.72 (0.68, 0.76)*	1.54 (1.40, 1.69)*	0.81 (0.70, 0.94)*	0.53 (0.42, 0.65)*
MTATP6	1.87 (1.25, 2.78)*	1.24 (0.73, 2.09)	0.66 (0.39, 1.14)	1.15 (0.57, 2.32)	0.83 (0.46, 1.50)	0.72 (0.34, 1.55)
UCP2	1.67 (1.07, 2.59)*	1.31 (1.15, 1.49)*	0.79 (0.58, 1.06)	2.06 (1.87, 2.26)*	1.20 (0.94, 1.53)	0.58 (0.58, 0.58)*
Endocrine hormones						
INS#	1.27 (0.91, 1.78)	1.31 (1.02, 1.68)*	1.03 (0.63, 1.68)	1.49 (1.08, 2.05)*	1.04 (0.99, 1.09)	0.70 (0.54, 0.91)*
SST†	1.09 (0.72, 1.63)	1.32 (1.03, 1.70)*	1.22 (0.73, 2.03)	1.37 (1.30, 1.44)*	0.85 (0.81, 0.89)*	0.62 (0.56, 0.69)*
Maintenance of cell populations						
IGF1‡	1.26 (1.16, 1.37)*	0.99 (0.86, 1.14)	0.78 (0.73, 0.85)*	1.86 (1.83, 1.90)*	1.21 (0.98, 1.50)	0.65 (0.52, 0.81)*
IGF2‡	1.16 (0.81, 1.66)	0.97 (0.88, 1.07)	0.84 (0.60, 1.17)	1.82 (1.71, 1.95)*	1.54 (1.07, 2.23)*	0.84 (0.72, 0.99)*
INSR	1.05 (0.97, 1.14)	0.83 (0.68, 1.02)	0.79 (0.66, 0.95)*	1.16 (0.82, 1.65)	0.93 (0.77, 1.12)	0.80 (0.60, 1.06)
IGF1R	0.92 (0.83, 1.02)	1.00 (0.72, 1.38)	1.08 (0.87, 1.34)	0.68 (0.50, 0.94)*	0.70 (0.68, 0.72)*	1.02 (0.75, 1.40)
FOXO1	1.20 (1.17, 1.23)*	1.02 (0.94, 1.10)	0.85 (0.81, 0.89)*	1.13 (0.73, 1.74)	1.28 (0.94, 1.74)	1.13 (0.69, 1.86)

Data are displayed as fold change (99% confidence intervals). If confidence intervals do not cross 1.0 (*), mRNA expression is statistically different from CON or FGRS at this level.

Female: CON, n=6-8; FGRS, n=5-8; FGRI, n=4-8; male: CON, n=5-8; FGRS, n=5-7; FGRI, n=6-8. Gene names (gene symbol): solute carrier family 2 member 2 (SLC2A2); glucokinase (GCK); potassium voltage-gated channel subfamily J member 11 (KCNJ11); transcription factor A (TFAM); nuclear respiratory factor 1 (NRF1); uncoupling protein 2 (UCP2); mitochondrially encoded ATP synthase membrane subunit 6 (MTATP6); insulin (INS); somatostatin (SST); insulin-like growth factor 1 (IGF1); insulin like growth factor 2 (IGF2); insulin receptor, β-

subunit (INSR); insulin like growth factor 1 receptor (IGF1R); forkhead box O1 (FOXO1). Gene names marked with symbols denote β-cell (#), δ-cell (†), or islet cell (‡) specific expression; genes without symbols are expressed across multiple cell types in whole-pancreas.

Table 3.

Skeletal muscle gene expression at 18-months of age.

	Female			Male		
Gene symbol	FGRS vs. CON	FGRI vs. CON	FGRI vs. FGRS	FGRS vs. CON	FGRI vs. CON	FGRI vs. FGRS
Insulin signalling						
INSR	0.78 (0.55, 1.11)	1.00 (0.69, 1.45)	1.27 (1.02, 1.59)*	0.86 (0.65, 1.14)	0.91 (0.74, 1.13)	1.06 (0.88, 1.28)
IRS1	0.92 (0.84, 1.02)	1.07 (1.00, 1.14)*	1.15 (0.99, 1.34)	0.91 (0.91, 0.92)*	0.83 (0.78, 0.89)*	0.91 (0.90, 0.92)*
PIK3CB	0.71 (0.46, 1.10)	0.88 (0.55, 1.39)	1.23 (0.79, 1.93)	0.93 (0.50, 1.71)	0.63 (0.33, 1.19)	0.68 (0.37, 1.22)
AKT2	0.94 (0.88, 1.00)*	1.01 (1.01, 1.01)*	1.07 (1.05, 1.10)*	0.96 (0.89, 1.03)	0.99 (0.99, 0.99)*	1.03 (1.00, 1.06)*
PRKCZ	0.93 (0.92, 0.94)*	0.99 (0.95, 1.03)	1.06 (0.95, 1.18)	0.81 (0.77, 0.85)*	0.86 (0.86, 0.86)*	1.07 (1.04, 1.09)*
SLC2A4	1.08 (1.02, 1.15)*	1.10 (0.97, 1.25)	1.02 (0.93, 1.12)	1.17 (1.05, 1.30)*	0.86 (0.78, 0.93)*	0.73 (0.60, 0.89)*
Mitochondria number and function						
PPARGC1A	0.76 (0.62, 0.93)*	0.85 (0.71, 1.01)	1.12 (0.95, 1.30)	1.04 (0.67, 1.59)	0.71 (0.44, 1.15)	0.69 (0.50, 0.94)*
TFAM	0.50 (0.37, 0.68)*	0.65 (0.55, 0.76)*	1.30 (0.83, 2.02)	0.65 (0.33, 1.27)	0.52 (0.26, 1.06)	0.80 (0.47, 1.38)
NRF1	0.70 (0.52, 0.93)*	0.91 (0.72, 1.16)	1.31 (1.21, 1.43)*	0.85 (0.73, 0.98)*	0.93 (0.81, 1.07)	1.10 (0.99, 1.23)
UCP2	0.85 (0.75, 0.96)*	0.80 (0.73, 0.88)*	0.94 (0.74, 1.21)	0.77 (0.70, 0.85)*	1.05 (0.99, 1.12)	1.37 (1.20, 1.57)*
MTATP6	0.81 (0.70, 0.93)*	0.92 (0.78, 1.09)	1.15 (0.83, 1.59)	1.14 (0.99, 1.32)	0.65 (0.58, 0.74)*	0.57 (0.56, 0.58)*
GPX	0.59 (0.58, 0.60)*	0.77 (0.77, 0.78)*	1.31 (1.11, 1.56)*	0.93 (0.91, 0.95)*	1.38 (1.27, 1.50)*	1.49 (1.37, 1.62)*
Growth factors						
IGF1	0.62 (0.45, 0.84)*	0.58 (0.56, 0.61)*	0.94 (0.53, 1.67)	0.71 (0.51, 0.98)*	0.95 (0.59, 1.53)	1.34 (1.07, 1.66)*
IGF2	0.88 (0.68, 1.13)	1.19 (0.92, 1.56)	1.34 (1.27, 1.46)*	1.10 (0.92, 1.33)	1.32 (1.17, 1.48)*	1.19 (1.04, 1.37)*
IGF1R	0.79 (0.56, 1.12)	1.07 (0.74, 1.54)	1.35 (1.11, 1.64)*	0.80 (0.65, 0.97)*	0.87 (0.72, 1.06)	1.10 (1.02, 1.18)*

Data are displayed as fold change (99% confidence intervals). If confidence intervals do not cross 1.0 (*), gene expression is statistically different from CON or FGRS at this level. Female: CON, n=8; FGRS, n=9; FGRI, n=8; male: CON, n=7-8; FGRS, n=7; FGRI, n=8. Gene names (gene symbol): insulin receptor, β-subunit (INSR); insulin receptor substrate 1 (IRS1); phosphatidylinositol-4,5-bisphosphate 3-kinase catalytic subunit beta (PIK3CB); AKT serine/threonine kinase 2 (AKT2); protein kinase c zeta (PRKCZ); solute carrier family 2 member 4 (SLC2A4); peroxisome proliferator activated receptor gamma coactivator 1 Alpha (PPARGC1A); transcription factor A (TFAM); nuclear respiratory factor 1 (NRF1); uncoupling

protein 2 (UCP2); mitochondrially encoded ATP synthase membrane subunit 6 (MTATP6); glutathione peroxidase (GPX); insulin-like growth factor 1 (IGF1); insulin like growth factor 2 (IGF2); insulin like growth factor 1 receptor (IGF1R).

Sexually dimorphic changes in the endocrine pancreas and skeletal muscle in young adulthood following intra-amniotic IGF-I treatment of growth-restricted fetal sheep

METHODS

1. Fetal growth restriction (FGR) induced via embolization (103-107 dGA)
2. Weekly intra-amniotic treatment (107-135 dGA)

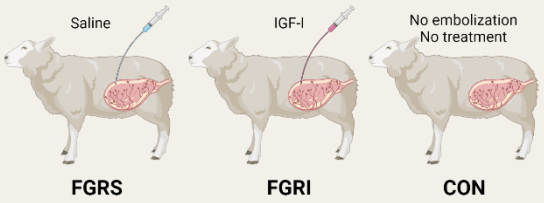

3. Lambs are born and maintained to 18-months of age
4. Tissue collection

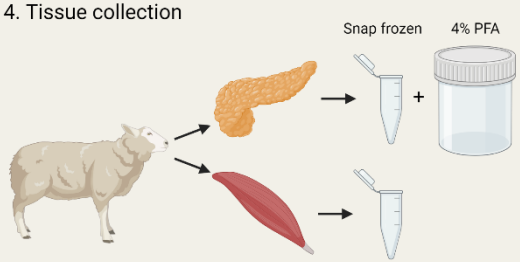

OUTCOME

Pancreatic endocrine cell mass
vs. CON

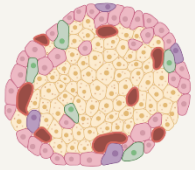

	♀ FGRS	♀ FGRI	♂ FGRS	♂ FGRI
β-cell mass	–	–	–	–
α-cell mass	–	–	–	↑↑↑
δ-cell mass	↑	↑	–	–

Whole pancreas gene expression
vs. CON

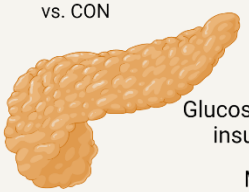

	♀ FGRS	♀ FGRI	♂ FGRS	♂ FGRI
Glucose-stimulated insulin secretion	–	–	↑	–
Mitochondria	↑	↑	↑	–

Skeletal muscle gene expression
vs. CON

	♀ FGRS	♀ FGRI	♂ FGRS	♂ FGRI
Insulin signaling	↓	–	↓	↓
Mitochondria	↓↓	↓	↓	–

CONCLUSION A brief period of intra-amniotic IGF-I treatment of fetal growth restriction had sex-specific developmental effects on glucose regulating pathways in the endocrine pancreas and skeletal muscle at the tissue and cellular levels that were present in young adulthood.